

Improved Methods for Broadband Outdoor Radiometer Calibration (BORCAL)

*S. M. Wilcox, A. Andreas, I. Reda, and Daryl Myers
National Renewable Energy Laboratory
Golden, Colorado*

Abstract

The Atmospheric Radiation Measurement (ARM) Program deploys approximately 100 radiometers to measure broadband solar radiation at stations in the North Slope of Alaska (NSA), Southern Great Plains (SGP), and Tropical Western Pacific (TWP) Cloud and Radiation Testbed (CART) sites. Two broadband outdoor radiometer calibration (BORCAL) events performed at the SGP radiometer calibration facility (RCF) each year maintain radiometer calibration traceability to the World Radiometric Reference and assure reliable and uniform measurements at each CART site. Calibrations are performed using the radiometer calibration and characterization (RCC) software developed by the National Renewable Energy Laboratory, allowing simultaneous calibrations of up to 200 instruments.

The first generation RCC installed in 1996 was developed and implemented on a DOS computing platform. Subsequent advances in operating systems and connectivity technology outdated the system's computing environment, and the system became difficult to maintain. These issues and recent improvements in radiometer calibration knowledge led to the upgrade of RCC to a Windows-based product with improved functionality and a more flexible user interface. This poster describes changes and functional improvements in the new system: a more comprehensive basis for calculating calibration uncertainty, accommodation of new state-of-the-art cavity radiometer reference instruments at the RCF, implementation of improved diffuse reference measurements, improved reporting of calibration results, the ability to perform tilt calibrations for increasing pyranometer angular response measurements, improved event configuration, and the capability to correct and document data acquisition or configuration errors.

BORCAL Configuration

Figures 1 and 2 show the enhanced BORCAL event configuration capabilities. In Figure 1, the hierarchical configuration schema is depicted. The operator starts with a configuration overview screen, from which system instruments (such as reference instruments, data logger, etc.) may be selected and test instruments configured. During the selection process, the system allows access to the instrument database, which provides easy access to instrument information. In Figure 2, the configuration is verified by following a set protocol in which operators work as a pair; one identifying the physical instrument at the calibration platform and the other identifying the configured instrument in the system. Ultimately, the instrument and its system configuration are directly related and confirmed by shading the physical instrument and watching the change in instrument voltage in the system.

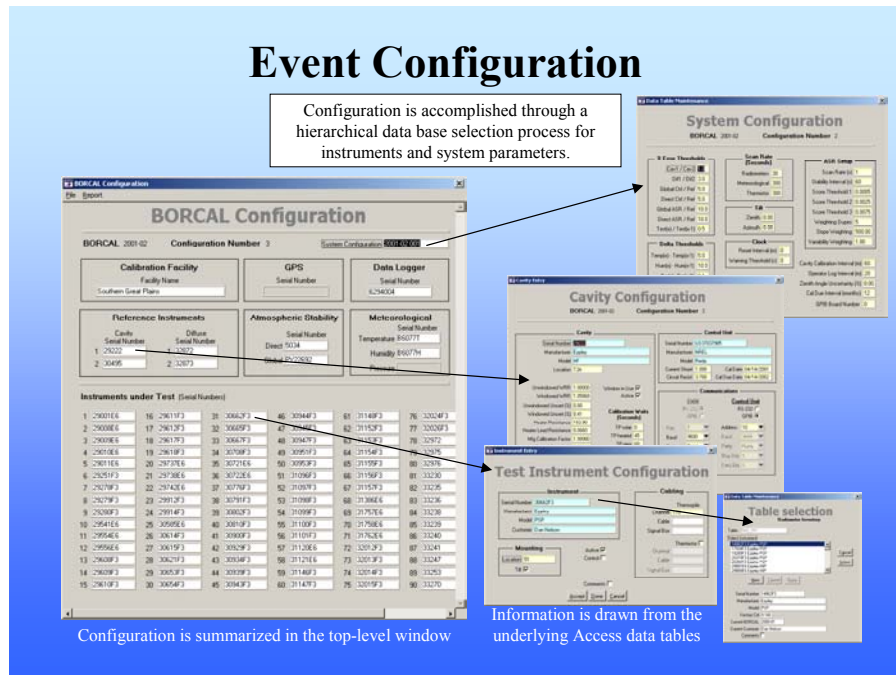


Figure 1.

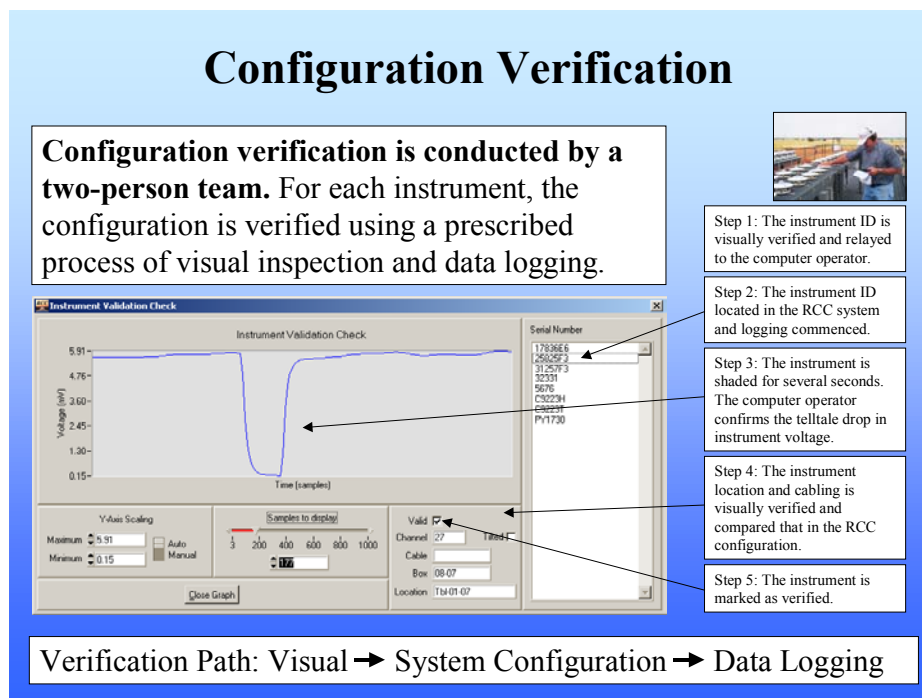


Figure 2.

Data Acquisition

Figure 3 shows an overview of the data acquisition, which includes extensive graphing and real-time error checking. Alarm conditions are identified, alerting the operator to resolve problems and minimize the amount of data collected under error conditions. This improves the quality of the data and reduces the uncertainty of the calibration results.

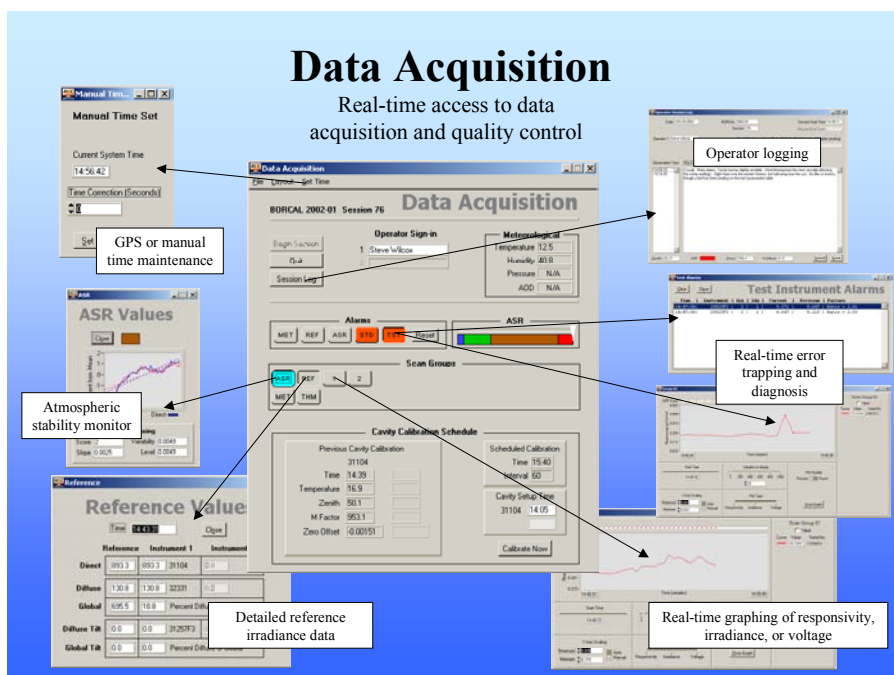


Figure 3.

Database Maintenance

All configuration, instrument, and results are stored in a Microsoft Access database. The system provides a suite of database maintenance tools for viewing data, configuration correction, and results analysis, as shown in Figure 4.

Calibration Calculations

Figures 5 and 6 show the reference irradiance sources for each type of calibration used for calculating instrument responsivity. Depending on the instrument, the reference irradiance comes from the cavity radiometer, the diffuse radiometer, or component summation technique of the two. Additional pyranometer characterizations are shown in Figure 7.

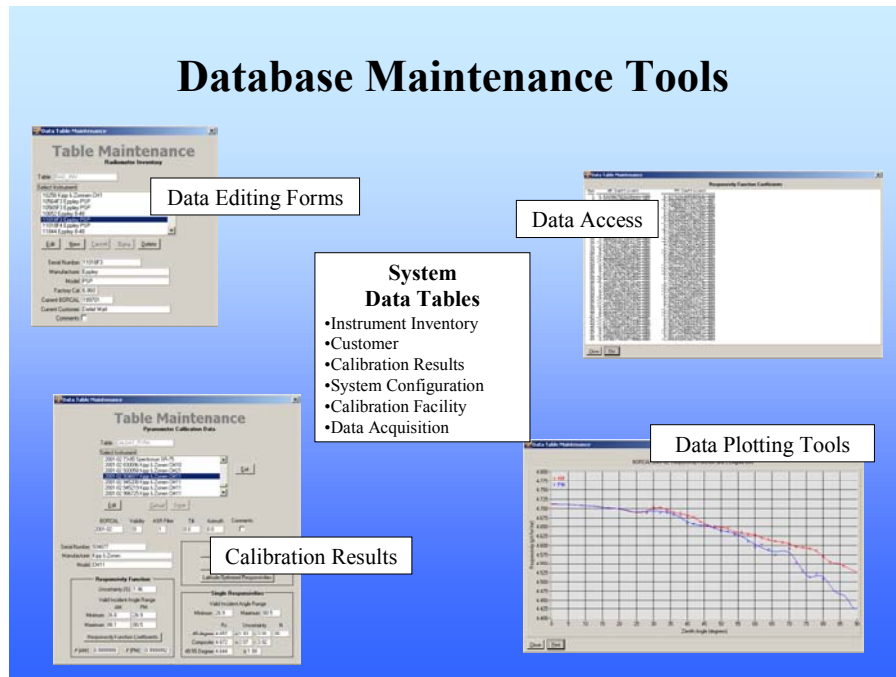


Figure 4.

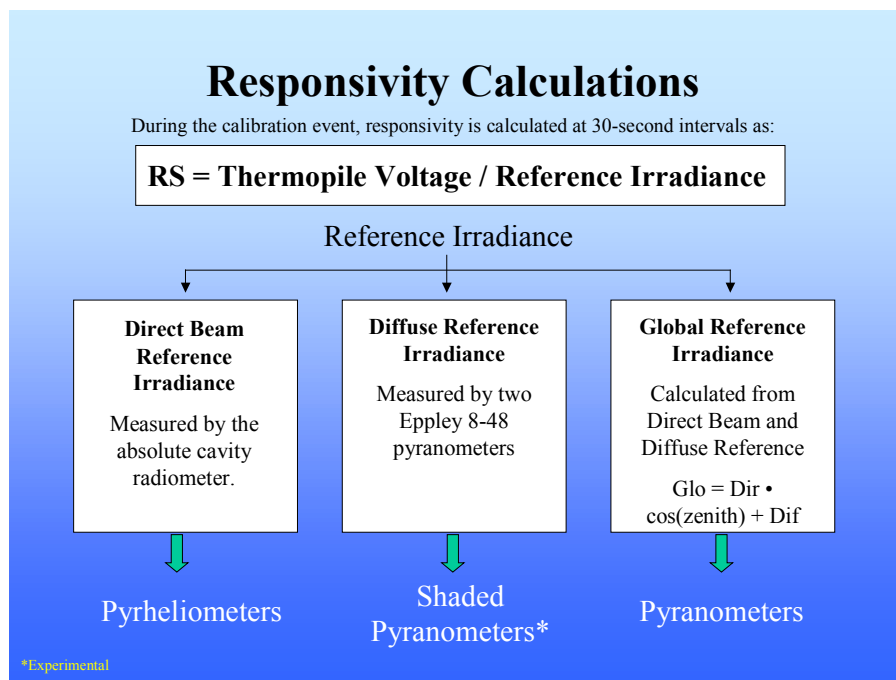


Figure 5.

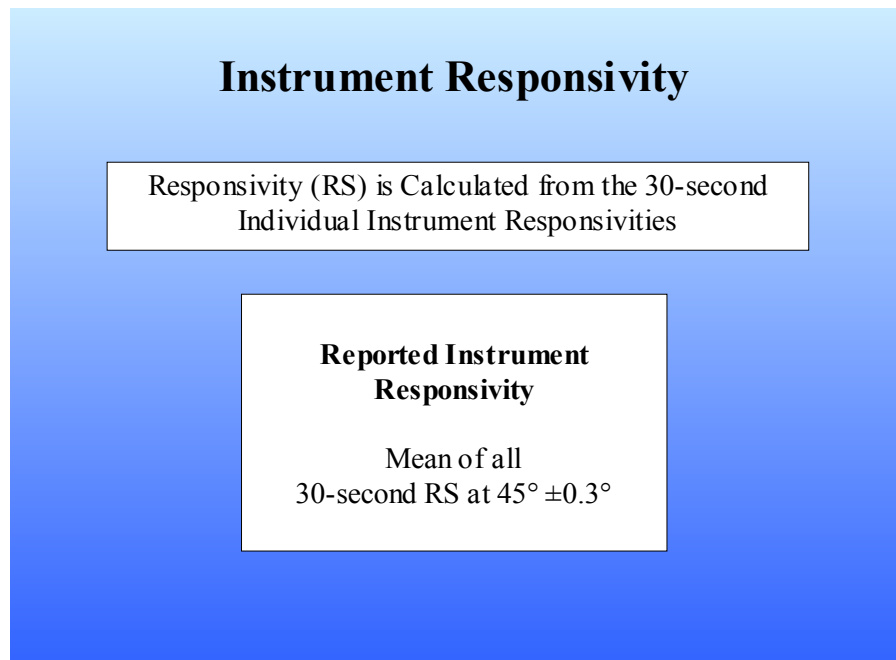


Figure 6.

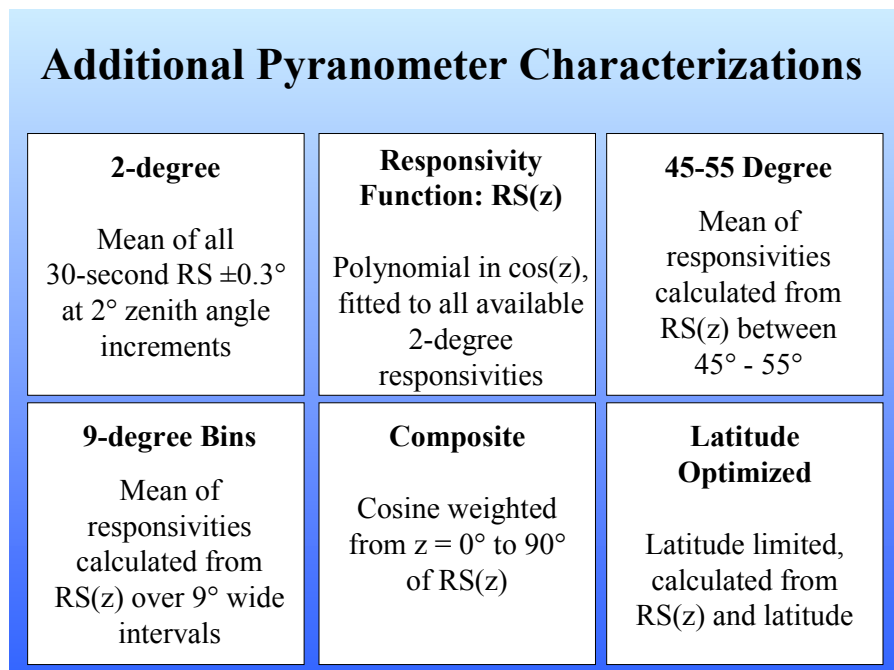


Figure 7.

Uncertainty Calculations

Figure 8 shows the sources of calibration uncertainty in the RCC process. These sources are different for pyranometers and pyrhemimeters. Figure 9 shows the calibration uncertainty calculations for pyranometers and pyrhemimeters respectively.

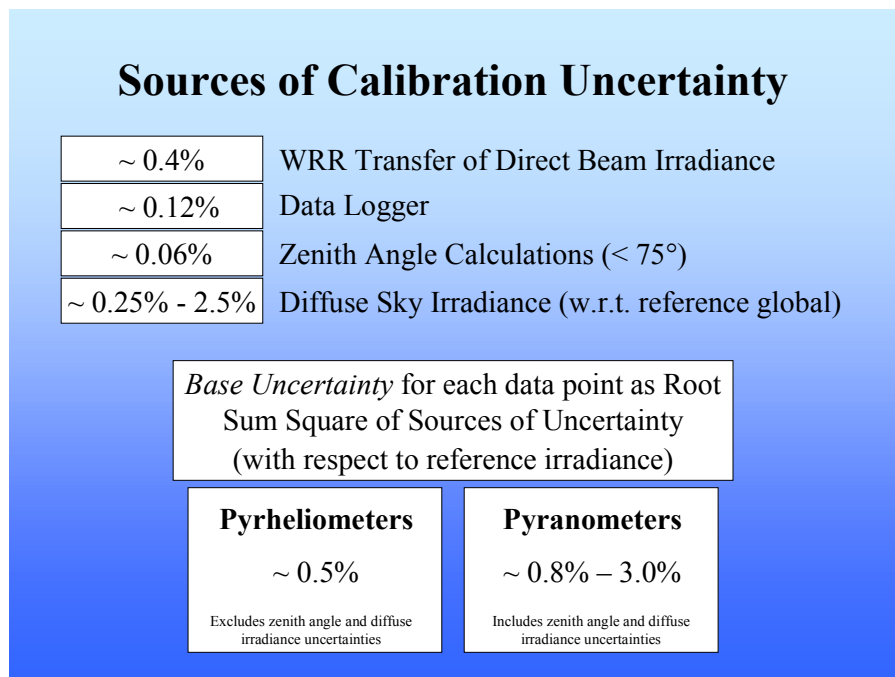


Figure 8.

Results and Reporting

The RCC system produces calibration certificates that conform to intraseasonal oscillations (ISO) guidelines. Sample certificates are shown in Figure 10. In addition to the calibration certificates, the RCC system produces suggested methods of applying the calibration results. The different methods are shown in Figure 11. As part of the need to distribute calibration results, the system has several built-in data exporting functions, including a customizable export that is compatible with common data format conventions. Examples of RCC exports are shown in Figure 12.

Results and Reporting

The RCC system produces calibration certificates that conform to ISO guidelines. Sample certificates are shown in Figure 10. In addition to the calibration certificates, the RCC system produces suggested methods of applying the calibration results. The different methods are shown in Figure 11. As part of the need to distribute calibration results, the system has several built-in data exporting functions, including a customizable export that is compatible with common data format conventions. Examples of RCC exports are shown in Figure 12.

Calibration Uncertainty

Calculated from 30-second data points

Terms

- U_{avg} = Mean of base uncertainties (%)
 U_{std} = Standard deviation, base uncertainties
 RS_{max} = Highest responsivity (within Z range)
 RS_{min} = Lowest responsivity (within Z range)
 RS = Mean responsivity @ 45°

Intermediate Calculations

- $U_{rad} = [U_{avg}^2 + (2 \cdot U_{avg})^2]^{1/2}$
 $E_+ = 100 \cdot (RS_{max} - RS) / RS$
 $E_- = 100 \cdot (RS - RS_{min}) / RS$

±Uncertainties (%)

- $U_{95+} = +(U_{rad} + E_+)$
 $U_{95-} = -(U_{rad} + E_-)$

Figure 9.

Calibration Certificates

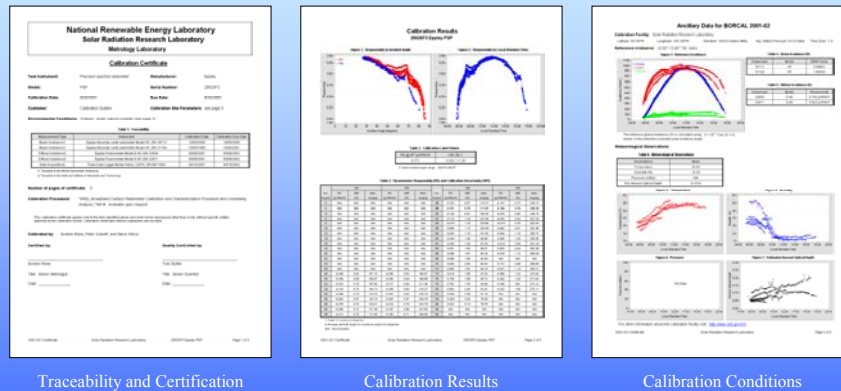


Figure 10.

Suggested Methods of Applying Results

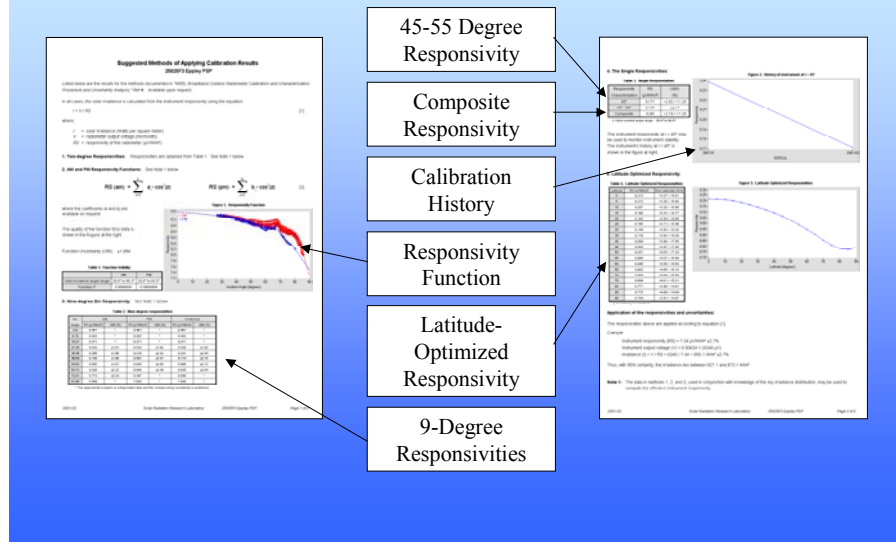


Figure 11.

Data Exporting and Distribution

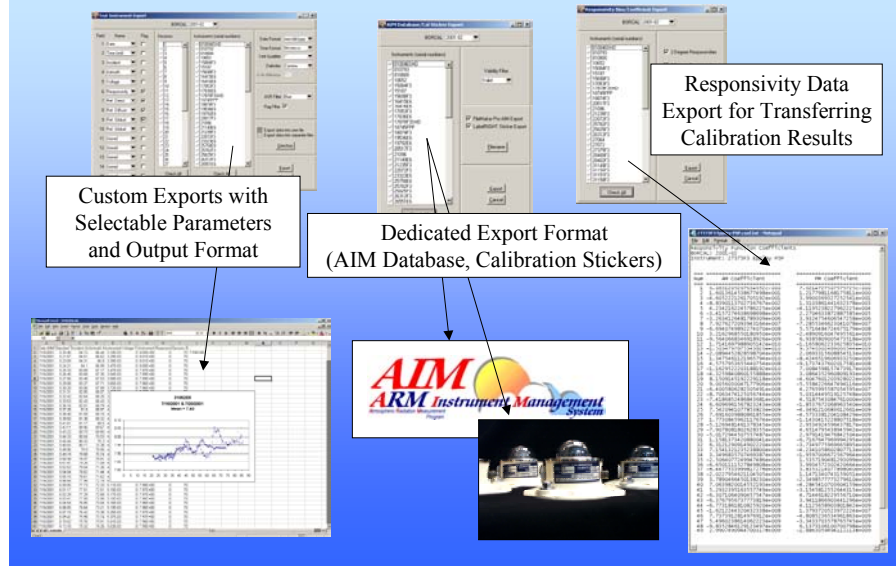


Figure 12.

Conclusions

The updated version of the Radiometer Calibration and Characterization System provides significant improvements over the DOS version:

- Calibration certificates using ISO guidelines
- Easier, more reliable configuration and error correction
- Greater capabilities for monitoring and control during data acquisition
- Improved calibration characterization and uncertainty analysis
- More flexibility in data reports, exports, and distribution.

Corresponding Author

S. M. Wilcox, Stephen_Wilcox@nrel.gov, (303) 275-4061

References

Myers, D. R., T. Stoffel, S. Wilcox, I. Reda, and A. Andreas, 2002: Recent Progress in Reducing the Uncertainty in and Improving Pyranometer Calibrations. *Journal of Solar Energy Engineering*, 124.

Myers, D. R., T. Stoffel, A. Andreas, S. Wilcox, and I. Reda, 2000: Improved Radiometric Calibrations and Measurements for Evaluating Photovoltaic Devices. 44 pp.; NREL TP-520-28941. National Renewable Energy Laboratory, Golden, Colorado.

Reda, I., and D. Myers, 1999: Calculating the Diffuse Responsivity of Solar Pyranometers. NREL Technical Report TP-560-26843. National Renewable Energy Laboratory, Golden, Colorado.

Reda, I., 1996: Calibration of an Absolute Cavity Radiometer with Traceability to the World Radiometric Reference. 79 p.; NREL Technical Report TP-463-20619. National Renewable Energy Laboratory, Golden, Colorado.

Stoffel, T. L., I. Reda, D. Myers, D. Rennè, S. Wilcox, J. Treadwell, 2000: Current Issues in Terrestrial Solar Radiation Instrumentation for Energy, Climate, and Space Applications.” *Metrologia*. In *Proceedings of the 7th International Conference on New Developments and Applications in Optical Radiometry (NEWRAD '99)*, October 25-27, 1999, Vol. 37(5), pp. 399-402. Madrid, Spain.

Wilcox, S. M., D. Myers, and I. Reda, 2002: Deriving a Latitude-optimized Pyranometer Calibration Factor. NREL/CP-560-31910. National Renewable Energy Laboratory, Golden, Colorado.

Wilcox, S. M., M. Bin Mahfoodh, N. Al-Abbadi, and D. Myers, 2001: Improving Global Solar Radiation Measurements Using Zenith Angle Dependent Calibration Factors. In *Proceedings of American Solar Energy Society Annual Conference, Forum 2001*, April 21-25, Washington D.C.

Wilcox, S. M., I. Reda, D. Nelson, and C. Webb, 1999: Traceability and verification of radiometer calibrations at the Southern Great Plains Radiometer Calibration Facility. . In *Proceedings of the Ninth Atmospheric Radiation Measurement (ARM) Science Team Meeting*, U.S. Department of Energy, Washington, D.C. Available URL:

http://www.arm.gov/docs/documents/technical/conf_9903/wilcox-99.pdf

Wilcox, S. M., and T. Stoffel, 1998: Radiometer calibrations at the ARM Southern Great Plains Radiometer Calibration Facility. In *Proceedings of the Ninth Atmospheric Radiation Measurement (ARM) Science Team Meeting*, U.S. Department of Energy, Washington, D.C.